Perturbation approach to resonance shifts of whispering-gallery modes in a dielectric microsphere as a probe of a surrounding medium

Iwao Teraoka and Stephen Arnold

Polytechnic University, Brooklyn, New York 11201

Frank Vollmer

Center for Studies in Physics and Biology, Rockefeller University, New York, New York 10021

Received September 5, 2002; revised manuscript received January 21, 2003

A first-order perturbation theory similar to the one widely used in quantum mechanics is developed for transverse-electric and transverse-magnetic photonic resonance modes in a dielectric microsphere. General formulas for the resonance frequency shifts in response to a small change in the exterior refractive index and its radial profile are derived. The formulas are applied to three sensor applications of the microsphere to probe the medium in which the sphere is immersed: a refractive-index detector, an adsorption sensor, and a refractive-index profile sensor. When they are applied to a uniform change in the refractive index in the surrounding medium, the formulas give the same results that one would obtain from the exact resonance equations for the two modes. In the application to adsorption of a thin layer onto the sphere surface, the results are identical to the first-order terms in the exact formulas obtained for the adsorption layer. In the last-named example, a scheme is proposed for instantaneous measurement of the refractive-index profile near the sphere's surface.

OCIS codes: 170.4520, 300.6490, 260.2110.

1. INTRODUCTION

Ever since it was suggested that microspheres coupled to optical fibers could be a particular sensitive system for the sensing of adsorbed molecules,[1] there has been increasing experimental support for using narrow-linewidth photonic resonance modes in a transparent microsphere as a probe of a surrounding medium.[2–4] A photon in one of these resonance modes [whispering gallery modes (WGMs)] is mostly confined to the interior of the sphere while it is traveling near the surface by total internal reflection. The photon orbits many times before being absorbed or exiting.[1,5–9] Recently Vollmer *et al.*[3] demonstrated that a silica microsphere in a buffer solution exhibits a large shift in resonance wavelength when protein molecules are adsorbed onto the sphere's surface. A single-layer adsorption of bovine serum albumin caused the wavelength to shift by approximately 16 parts in 10^6. Resonances were detected from dips in the transmission through an eroded fiber that was coupled evanescently to the microsphere. The eroded fiber was prepared by removal of most of the cladding to expose the evanescent field.

As the experiment of Vollmer *et al.* demonstrated, the resonance frequency is sensitive to the environment in close vicinity to the sphere surface. Any change in the vicinity can be detected as a frequency shift. The changes will include adsorption of molecules onto the sphere's surface and change of concentration in the surrounding solution.

Following the experiment, Arnold *et al.*[4] presented a perturbation approach to evaluating the resonance frequency shift of a WGM. In their formulation, frequency shift $\delta\omega$ was associated with the perturbation in energy δE of a single-photon resonant state that is due to adsorption of a dielectric nanoparticle by

$$\hbar\,\delta\omega = \delta E = {}^1/_2\,\mathrm{Re}(\delta\mathbf{p}\cdot\mathbf{E}^*), \tag{1}$$

where $\delta\mathbf{p}$ is the induced dipole moment in the nanoparticle and $\mathbf{E}$ is local field within the original mode. The formulation was applied to a microsphere with monolayer coverage by protein molecules and to a sphere with a single protein molecule adsorbed onto the equator. The authors predicted protein, sphere, and optical parameters for the detection of a single protein molecule.

In the past, a perturbation approach was applied to resonance modes in a spherical microcavity with a reflective interior surface.[10,11] Formulas were obtained for the frequency shift caused by a spatial change in the refractive index within the microcavity. A more rigorous perturbation theory was presented by Lai *et al.*[12] to treat the effect of isotropic and anisotropic deformations of the sphere surface on the resonance frequency shift without changing the refractive index in the exterior or in the interior of the sphere.

The aforementioned formulations, however, do not allow one to evaluate the frequency shift that is due to changes in the medium surrounding the microsphere. In this paper we derive formulas for frequency shifts that are due to these changes within a rigorous theoretical framework. The perturbation that we consider is a small change in the refractive index. The change can be either within the sphere or in the surrounding medium. When

it is applied to a uniform change in the refractive index of the surrounding medium, the formula gives the same result as that obtained from the resonance formula for a homogeneous sphere.

The formulas and examples presented here should lay the groundwork for sensor applications of WGMs for refractive-index sensing. We focus on the frequency shift, because it can be measured accurately (the resolution is better than 1/50 of the linewidth[4]) and is relatively unaffected by auxiliary effects that are important in linewidth measurements, such as scattering and absorption by inhomogeneity of the sphere and the surrounding medium. First we derive general formulas for the frequency shifts for TE and TM modes. Then we apply these formulas to uniform refractive-index changes in the surround, to the adsorption layer, and to the refractive index profile near the surface.

We describe our theory following the formulation that Johnson[13] presented to explain resonance states in a microsphere. His notation will be followed as much as possible. Unlike in his system, for which the exterior medium is air, in our calculations the medium that surrounds the sphere has a refractive index between that of a sphere and that of vacuum.

2. WAVE EQUATIONS

In the absence of continuous energy flow into the sphere a WGM loses its energy in a finite lifetime. In effect, the frequency of the WGM is complex.[12] With a continuous influx of energy to match the loss, a steady-state mode can be maintained with a real frequency. The two modes are only slightly different, as manifested by the fact that the imaginary part of the frequency in the decaying mode is much smaller than the real part.[12] We stick to the steady-state mode here for simplicity.

The wave of a WGM is specified by vacuum wave vector k, angular momentum quantum number l, and another quantum number μ ($\mu = -l, -l+1, ..., l$). We assume that refractive index $m(r)$ depends solely on radial distance r from the sphere center. Amplitude $\mathbf{E}$ of the electric field satisfies the following vector differential equation:

$$\nabla \times \nabla \times \mathbf{E} - k^2 m^2(r)\mathbf{E} = 0. \tag{2}$$

Introduction of scalar functions $S_l(r, k)$ and $T_l(r, k)$ for the TE and TM modes, respectively, simplifies Eq. (2), as will be shown below. For the TE mode, electric field $\mathbf{M}_{l\mu}(r, \theta, \varphi)$ in spherical polar coordinates is specified by l and μ and is given as[13]

$$\mathbf{M}_{l\mu}(r, \theta, \varphi) = \frac{\exp(i\mu\varphi)}{kr} S_l(r, k)\mathbf{X}_{l\mu}(\theta). \tag{3}$$

For the TM mode, electric field $\mathbf{N}_{l\mu}(r, \theta, \varphi)$ is given as

$$\mathbf{N}_{l\mu}(r, \theta, \varphi) = \frac{\exp(i\mu\varphi)}{k^2 m^2(r)}\left[\frac{1}{r}\frac{\partial}{\partial r} T_l(r, k)\mathbf{Y}_{l\mu}(\theta) + \frac{T_l(r, k)}{r^2}\mathbf{Z}_{l\mu}(\theta)\right]. \tag{4}$$

Here the angular functions $\mathbf{X}_{l\mu}(\theta)$, $\mathbf{Y}_{l\mu}(\theta)$, and $\mathbf{Z}_{l\mu}(\theta)$ are expressed as[14]

$$\mathbf{X}_{l\mu}(\theta) = i\pi_{l\mu}(\theta)\hat{e}_\theta - \tau_{l\mu}(\theta)\hat{e}_\varphi, \tag{5a}$$

$$\mathbf{Y}_{l\mu}(\theta) = \tau_{l\mu}(\theta)\hat{e}_\theta + i\pi_{l\mu}(\theta)\hat{e}_\varphi, \tag{5b}$$

$$Z_{l\mu}(\theta) = l(l+1)P_l{}^{\mu}(\cos\theta)\hat{e}_r, \tag{5c}$$

where $\hat{e}_r$, $\hat{e}_\theta$, and $\hat{e}_\varphi$ are the unit vectors in the relevant directions, $P_l{}^{\mu}(x)$ is the associated Legendre function, and $\pi_{l\mu}(\theta)$ and $\tau_{l\mu}(\theta)$ are defined as

$$\pi_{l\mu}(\theta) = \frac{\mu}{\sin\theta} P_l{}^{\mu}(\cos\theta), \tag{6a}$$

$$\tau_{l\mu}(\theta) = \frac{\partial}{\partial\theta} P_l{}^{\mu}(\cos\theta). \tag{6b}$$

TE mode scalar function $S_l(r, k)$ is a solution of a Schrödinger-equation-like differential equation:

$$\left[-\frac{\partial^2}{\partial r^2} + V_{\mathrm{TE}}(r, k) + \frac{l(l+1)}{r^2}\right] s_l(r, k) = k^2 S_l(r, k). \tag{7}$$

The potential $V_{\mathrm{TE}}(r, k)$ is given as

$$V_{\mathrm{TE}}(r, k) = k^2[1 - m^2(r)]. \tag{8}$$

The TM mode scalar function $T_l(r, k)$ is a solution of a slightly different equation:

$$\left[-\frac{\partial^2}{\partial r^2} + V_{\mathrm{TM}}(r, k) + \frac{l(l+1)}{r^2}\right] T_l(r, k) = k^2 T_l(r, k), \tag{9}$$

where the potential $V_{\mathrm{TM}}(r, k)$ is given as

$$V_{\mathrm{TM}}(r, k) = V_{\mathrm{TE}}(r, k) + \frac{2}{m(r)}\frac{\mathrm{d}m}{\mathrm{d}r}\frac{\mathrm{d}}{\mathrm{d}r}. \tag{10}$$

When a dielectric microsphere of radius a with uniform refractive index m_1 is suspended in a uniform medium of refractive index m_2 with $m_1 > m_2$, i.e., when

$$V_{\mathrm{TE}}(r, k) = \begin{cases} k^2(1 - m_1{}^2) & (r < a) \\ k^2(1 - m_2{}^2) & (r > a) \end{cases}, \tag{11}$$

the solution of Eq. (7) is expressed by spherical Ricatti–Bessel functions $\psi_l(z)$ and $\chi_l(z)$, defined as

$$\psi_l(z) = z j_l(z), \qquad \chi_l(z) = z n_l(z), \tag{12}$$

where $j_l(z)$ and $n_l(z)$ are the lth spherical Bessel function and the lth spherical Neumann function, respectively. The solution of the TE mode is given as

$$S_l(r, k) = \begin{cases} \psi_l(m_1 kr) \\ B_l(k)\phi_l(m_2 kr) \end{cases}, \tag{13}$$

where $B_l(k)$ is a constant of r and, for a given k,

$$\phi_l(m_2 kr) = \chi_l(m_2 kr) + \beta_l(k)\psi_l(m_2 kr), \tag{14}$$

where $\beta_l(k)$ is a constant of r. Continuity of the tangential component of the electric field and of the normal component of the electric displacement requires that

$$\psi_l(m_1 ka) = B_l(k)\phi_l(m_2 ka), \tag{15a}$$

$$m_1\psi_l'(m_1 ka) = B_l(k)m_2\phi_l'(m_2 ka), \tag{15b}$$

where the prime denotes the derivative with respect to the argument, and the derivative is taken at a constant k. At resonance, wave vector k_0 satisfies $\beta_l(k_0) = 0$. Together with the boundary condition, the resonance of the TE mode is specified by

$$m_1\frac{\psi_l'(m_1k_0a)}{\psi_l(m_1k_0a)} = m_2\frac{\chi_l'(m_2k_0a)}{\chi_l(m_2k_0a)}. \tag{16}$$

This equation is solved for k_0a. The solutions are bound from l/m_1 to l/m_2.[13] For given m_1 and m_2 there may be more than one solution. These modes are called the first-order mode ($n = 1$), the second-order mode ($n = 2$), etc. with increasing magnitude of k_0a. The solutions are real.

TM solution $T_l(r, k)$ is also given by Eq. (13), as V_{TM} is identical to V_{TE} in the interior of and exterior to the sphere. We use a different coefficient:

$$T_l(r, k) = \begin{cases} \psi_l(m_1kr) \\ A_l(k)\phi_l(m_2kr), \end{cases} \tag{17}$$

where $A_l(k)$ is a constant of r and

$$\phi_l(m_2kr) = \chi_l(m_2kr) + \alpha_l(k)\psi_l(m_2kr), \tag{18}$$

where $\alpha_l(k)$ is a constant of r. The boundary condition of the electric field leads to

$$\psi_l(m_1ka) = A_l(k)\phi_l(m_2ka), \tag{19a}$$

$$\psi_l'(m_1ka)/m_1 = A_l(k)\phi_l'(m_2ka)/m_2. \tag{19b}$$

There is a jump in $\partial T_l(r, k)/\partial_r$ at the interface, because V_{TM} has a jump at $r = a$. At resonance, wave vector k_0 satisfies $\alpha_l(k_0) = 0$. The resonance of the TM mode is specified by

$$\frac{1}{m_1}\frac{\psi_l'(m_1k_0a)}{\psi_l(m_1k_0a)} = \frac{1}{m_2}\frac{\chi_l'(m_2k_0a)}{\chi_1(m_2k_0a)}. \tag{20}$$

3. ORTHOGONALITY

The solutions for the TE modes and for the TM modes have different orthogonalities. First we consider the orthogonality of $S_l(r, k)$ with various values of k. Let us examine the integral given as

$$\int_0^\infty S_l(r, k)S_l(r, k_a)m^2(r)\mathrm{d}r$$
$$= {m_1}^2\int_0^a \psi_l(m_1kr)\psi_l(m_1k_ar)\mathrm{d}r$$
$$+ B_l(k)B_l(k_a){m_2}^2\int_a^\infty \phi_l(m_2kr)\phi_l(m_2k_ar)\mathrm{d}r \tag{21}$$

for $k \neq k_a$. The integrand in the second term is a sinusoidal function in the asymptote of $r \to \infty$. Introduction of the convergence coordinate forces the integral at $r \to \infty$ to vanish. Using Eqs. (C1) and (C3) below, we obtain

$$\int_0^\infty S_l(r, k)S_l(r, k_a)m^2(r)\mathrm{d}r$$
$$= \frac{m_1}{k^2 - {k_a}^2}[-k\psi_l'(m_1ka)\psi_l(m_1k_aa)$$
$$+ k_a\psi_l(m_1ka)\psi_l'(m_1k_aa)] - \frac{m_2}{k^2 - {k_a}^2}B_l(k)B_l(k_a)$$
$$\times [-k\phi_l'(m_2ka)\phi_l(m_2k_aa)$$
$$+ k_a\phi_l(m_2ka)\phi_l'(m_2k_aa)]. \tag{22}$$

Use of Eqs. (15) leads to

$$\int_0^\infty S_l(r, k)S_l(r, k_a)m^2(r)\mathrm{d}r = 0. \tag{23}$$

Thus $S_l(r, k)$ of various values of k are orthogonal in this functional space under the TE boundary condition. We write it as follows:

$$\langle S_l(r, k)|m^2(r)|S_l(r, k_a)\rangle = 0, \tag{24}$$

where

$$\langle f|p|g\rangle \equiv \int f(r)p(r)g(r)\mathrm{d}r. \tag{25}$$

We might simplify Eq. (24) to

$$\langle k|m^2|k_a\rangle = 0. \tag{26}$$

The orthogonality is slightly different for TM modes. Its boundary condition makes

$$\int_0^\infty T_l(r, k)T_l(r, k_a)\mathrm{d}r$$
$$= \int_0^a \psi_l(m_1kr)\psi_l(m_1k_ar)\mathrm{d}r + A_l(k)A_l(k_a)$$
$$\times \int_0^\infty \phi_l(m_2kr)\phi_l(m_2k_ar)\mathrm{d}r \tag{27}$$

disappear when $k \neq k_a$. We write it as

$$\langle T_l(r, k)|T_l(r, k_a)\rangle = \langle k|k_a\rangle = 0, \tag{28}$$

where

$$\langle f|g\rangle \equiv \int f(r)g(r)\mathrm{d}r. \tag{29}$$

We can extend the above integrals to $k = k_a$. When the two waves have the same wave vectors, the integrand has a dc component, and the integral diverges. However, we can circumvent this behavior by first evaluating the integral for slightly different wave vectors with a convergence coordinate and then bringing the two wave vectors to the same value. Details of the calculation are given in Appendix A. From Eq. (A9) below,

$$\langle k_0|m^2|k_0\rangle = {\psi_l}^2\frac{a}{2}({m_1}^2 - {m_2}^2), \tag{30}$$

where $\psi_l = \psi_l(m_1k_0a)$. Likewise, for the TM mode, we have from Eq. (A10)

$$\langle k_0|k_0\rangle = \frac{a}{2}{\psi_l}^2\left(\frac{{m_1}^2}{{m_2}^2} - 1\right)\left[\left(\frac{\chi_l'}{\chi_l}\right)^2 + \frac{l(l+1)}{(m_1ka)^2}\right]. \tag{31}$$

Another way to avoid the divergence of the integrals in Eqs. (30) and (32) below is to place a large hypothetical concentric sphere with a reflective interior surface and evaluate the integrals for a WGM sustained in the large sphere. This method was adopted by Lai *et al.*[12]

Equations (3) and (4) relate $S_l(r, k)$ and $T_l(r, k)$ to electric field $\mathbf{M}$ of the TE mode and to field $\mathbf{N}$ of the TM mode, respectively. By integrating the electric energy densities divided by vacuum permittivity $m^2\mathbf{M}^2/2$ and $m^2\mathbf{N}^2/2$ over the entire space, we find that $\langle k|m^2|k\rangle$ and $\langle k|k\rangle$ essentially represent the total energy of the two modes.

4. FIRST-ORDER PERTURBATION FOR A FREQUENCY SHIFT

Now we consider a frequency shift when the system experiences a small change $\delta m(r)$ in its refractive index. We assume that the change depends on r only. The change can be either within the sphere or in the surrounding medium, although our interest is in the surrounding medium.

The unperturbed Hamiltonian for a TE wave with wave vector k_0 is given by

$$H_{\mathrm{TE},0}(k_0) = -\frac{\partial^2}{\partial r^2} + \left[V_{\mathrm{TE}}(r, k_0) + \frac{l(l+1)}{r^2} \right]. \quad (32)$$

The Schrödinger equation is

$$H_{\mathrm{TE},0}(k_0) S_0 = {k_0}^2 S_0, \quad (33)$$

where $S_0 = S_l(r, k_0)$ is the unperturbed solution.

When the refractive-index changes by an amount $\delta m(r)$, k_0 changes to $k_0 + \delta k$; the solution changes to $S_0 + \delta S$, and the potential function changes to $V_{\mathrm{TE}}(r, k_0) + \delta V_{\mathrm{TE}}$, where

$$\delta V_{\mathrm{TE}} = 2k_0 \delta k (1 - m^2) - 2{k_0}^2 m \, \delta m. \quad (34)$$

The perturbed Schrödinger equation is

$$[H_{\mathrm{TE},0}(k_0) + \delta V_{\mathrm{TE}}](S_0 + \delta S) = (k_0 + \delta k)^2 (S_0 + \delta S). \quad (35)$$

Collecting the first-order terms, we have

$$H_{\mathrm{TE},0}(k_0) \delta S + \delta V_{\mathrm{TE}} S_0 = {k_0}^2 \delta S + 2k_0 \delta k S_0. \quad (36)$$

We express δS as a superposition of $S_l(r, k)$ of different values of k, each of which is a solution of $H_{\mathrm{TE},0}(k)$:

$$\delta S = \sum_k c_k S_l(r, k), \quad (37)$$

where c_k is the superposition coefficient. Substituting δS into Eq. (36) with Eq. (37) and rearranging the result, we obtain

$$\sum_k c_k k^2 S_l(r, k) + \sum_k c_k [H_{\mathrm{TE},0}(k_0) - H_{\mathrm{TE},0}(k)] S_l(r, k) + \delta V_{\mathrm{TE}} S_l(r, k_0) = {k_0}^2 \sum_k c_k S_l(r, k) + 2k_0 \delta k S_l(r, k_0), \quad (38)$$

where

$$H_{\mathrm{TE},0}(k_0) - H_{\mathrm{TE},0}(k) = ({k_0}^2 - k^2)[1 - m^2(r)]. \quad (39)$$

We multiply Eq. (38) by $S_l(r, k_b)$ and integrate the product. Using the orthogonality of $S_l(r, k)$, we arrive at

$$-c_{k_b}({k_0}^2 - {k_b}^2)\langle k_b | m^2 | k_b \rangle + \langle k_b | \delta V_{\mathrm{TE}} | k_0 \rangle = 2k_0 \delta k \langle k_b | k_0 \rangle. \quad (40)$$

We obtain the first-order correction to the eigenvalue by setting k_b to k_0:

$$\langle k_0 | \delta V_{\mathrm{TE}} | k_0 \rangle = 2k_0 \delta k \langle k_0 | k_0 \rangle. \quad (41)$$

For δV_{TE} given by Eq. (34) we obtain the following formula:

$$\left(\frac{\delta k}{k_0} \right)_{\mathrm{TE}} = -\frac{\langle k_0 | m \, \delta m | k_0 \rangle}{\langle k_0 | m^2 | k_0 \rangle}. \quad (42)$$

The first-order correction to the eigenfunction can be obtained from Eq. (40).

The frequency shift of the TM mode is calculated in a similar way. The perturbation now has an additional term:

$$\delta V_{\mathrm{TM}} = \delta V_{\mathrm{TE}} + 2 \frac{\mathrm{d}(\delta m/m)}{\mathrm{d}r} \frac{\mathrm{d}}{\mathrm{d}r}. \quad (43)$$

We can invoke the orthogonality of eigenfunctions $T_l(r, k)$ by multiplying the counterpart of Eq. (38) by $m^{-2}(r) T_l(r, k)$. The first-order eigenvalue correction is obtained as

$$\left(\frac{\delta k}{k_0} \right)_{\mathrm{TM}} = -\frac{\langle k_0 | m^{-1} \delta m | k_0 \rangle}{\langle k_0 | k_0 \rangle} + \frac{\left\langle k_0 \left| \frac{1}{{k_0}^2 m^2} \frac{\mathrm{d}(\delta m/m)}{\mathrm{d}r} \frac{\mathrm{d}}{\mathrm{d}r} \right| k_0 \right\rangle}{\langle k_0 | k_0 \rangle}, \quad (44)$$

where $|k_0\rangle = T_0 = T_l(r, k_0)$ is the unperturbed solution. If δm vanishes rapidly toward $r = 0$ and $r = \infty$, it can be rewritten as

$$\left(\frac{\delta k}{k_0} \right)_{\mathrm{TM}} = -\frac{1}{{k_0}^2} \langle k_0 | k_0 \rangle^{-1} \int \frac{\delta m}{m^3} \times \left[\left(\frac{\mathrm{d}T_0}{\mathrm{d}r} \right)^2 + \frac{l(l+1)}{r^2} {T_0}^2 \right] \mathrm{d}r. \quad (45)$$

The two formulas, Eqs. (42) and (44) [or Eq. (45)], have a form the same as that of Eq. (1):

$$\frac{\delta k}{k_0} = -\frac{(\text{energy perturbation})}{2 \times (\text{electric energy})}. \quad (46)$$

We divide by 2 because the electric field energy changes by perturbation in m but the magnetic field energy does not.[4]

5. APPLICATIONS

Now we apply the general formulas to frequency shifts of a WGM by environmental changes, i.e., $\delta m_2(r)$. Other parameters (a and m_1) are assumed not to change, unless otherwise noted. Specifically, the following three cases are considered: (A) a uniform change in m_2 to be caused, for instance, by a change in the surrounding fluid, (B) addition of a thin layer with a different refractive index onto the sphere surface, and (C) a refractive-index profile near the sphere's surface.

A. Uniform Change in m_2

For a uniform change Δm_2 in the exterior refractive index we can also estimate the shift by using the resonance condition. A comparison of the result thus obtained with the one to be obtained from our general formulas for first-order perturbation will validate the general formulas. In Eq. (16), which gives the resonance condition for the TE

mode, we change k_0 to $k_0 + \Delta k$ and m_2 to $m_2 + \Delta m_2$. Collecting the first-order terms, we calculate fractional shift $\Delta k/k_0$ as

$$\left(\frac{\Delta k}{k_0}\right)_{\mathrm{TE}} = -\frac{m_2 \Delta m_2}{{m_1}^2 - {m_2}^2} \times \left[\frac{l(l+1)}{(m_2 k_0 a)^2} - 1 + \frac{1}{m_2 k_0 a}\frac{\chi_l'}{\chi_l} - \left(\frac{\chi_l'}{\chi_l}\right)^2\right] = -\frac{m_2 \Delta m_2}{{m_1}^2 - {m_2}^2}\left[\frac{\chi_{l+1}\chi_{l-1}}{{\chi_l}^2} - 1\right], \tag{47}$$

where Eq. (C6) below was used and $\chi_{l-1}(z)$, $\chi_l(z)$, and $\chi_{l+1}(z)$ are evaluated at $z = m_2 k_0 a$. For the TM mode, use of Eq. (20) leads to

$$\left(\frac{\Delta k}{k_0}\right)_{\mathrm{TM}} = -\frac{m_2 \Delta m_2}{{m_1}^2 - {m_2}^2} \times \frac{\dfrac{l(l+1)}{(m_2 k_0 a)^2} - 1 - \dfrac{1}{m_2 k_0 a}\dfrac{\chi_l'}{\chi_l} - \left(\dfrac{\chi_l'}{\chi_l}\right)^2}{\dfrac{l(l+1)}{(m_1 k_0 a)^2} + \left(\dfrac{\chi_l'}{\chi_l}\right)^2}. \tag{48}$$

Now we use the general formulas in the first-order perturbation to evaluate the fractional frequency shift. For the TE mode,

$$\langle k_0|m\,\delta m|k_0\rangle = m_2 \Delta m_2 [B_l(k_0)]^2 \int_a^\infty [\chi_l(m_2 k_0 r)]^2 \mathrm{d}r = [B_l(k_0)]^2 \frac{a}{2} m_2 \Delta m_2 \times \left\{-{\chi_l}'^2 + \left[\frac{l(l+1)}{(m_2 k_0 a)^2} - 1\right]\chi_l^2 + \frac{\chi_l \chi_l'}{m_2 k_0 a}\right\}, \tag{49}$$

where the same process that we used in evaluating Eq. (A9) below was used to force the integral to converge. With Eq. (30) we obtain the same equation as with Eq. (47).

For the TM mode we need to use the formula given by Eq. (44) because $\delta m(r)$ remains finite at large r. The integrals are evaluated as follows:

$$\langle k_0|m^{-1}\delta m|k_0\rangle = [A_l(k_0)]^2 \frac{a}{2}\frac{\Delta m_2}{m_2} \times \left\{-{\chi_l}'^2 + \left[\frac{l(l+1)}{(m_2 k_0 a)^2} - 1\right]\chi_l^2 + \frac{\chi_l \chi_l'}{m_2 k_0 a}\right\}, \tag{50}$$

$$\langle k_0|\frac{1}{{k_0}^2 m^2}\frac{\mathrm{d}(\delta m/m)}{\mathrm{d}r}\frac{\mathrm{d}}{\mathrm{d}r}|k_0\rangle = \frac{\Delta m_2}{{k_0}^2 m_2}\int_0^\infty \frac{1}{m^2} T_0 \frac{\mathrm{d}T_0}{\mathrm{d}r}\,\delta(r-a)\mathrm{d}r = \frac{\Delta m_2}{k_0 {m_2}^2}[A_l(k_0)]^2 \chi_l \chi_l'. \tag{51}$$

With formula (31) and Eq. (44) we obtain the same expression as with Eq. (48).

When $k_0 a \gg 1$, use of formulas (B5) and (B7) below simplifies Eqs. (47) and (48) to

$$\left(\frac{\Delta k}{k_0}\right)_{\mathrm{TE}} \cong -\frac{m_2 \Delta m_2}{{m_1}^2 - {m_2}^2}\left[\left(l + \frac{1}{2}\right)^2 - (m_2 k_0 a)^2\right]^{-1/2}, \tag{52}$$

$$\left(\frac{\Delta k}{k_0}\right)_{\mathrm{TM}} \cong -\frac{m_2 \Delta m_2}{{m_1}^2 - {m_2}^2} \frac{2(l+{}^1\!/_2)^2/(m_2 k_0 a)^2 - 1}{[(l+{}^1\!/_2)^2 - (m_2 k_0 a)^2]^{1/2}\left[\dfrac{(l+{}^1\!/_2)^2}{(m_1 k_0 a)^2} + \dfrac{(l+{}^1\!/_2)^2}{(m_2 k_0 a)^2} - 1\right]}. \tag{53}$$

The shift occurs in the same direction for the two modes. For the first-order mode $l \cong m_1 k_0 a$, and these expressions are further simplified to

$$\left(\frac{\Delta k}{k_0}\right)_{\mathrm{TE}} \cong -\frac{m_2 \Delta m_2}{({m_1}^2 - {m_2}^2)^{3/2}}\frac{1}{k_0 a}, \tag{54}$$

$$\left(\frac{\Delta k}{k_0}\right)_{\mathrm{TM}} \cong -\frac{m_2 \Delta m_2}{({m_1}^2 - {m_2}^2)^{3/2}}\left(2 - \frac{{m_2}^2}{{m_1}^2}\right)\frac{1}{k_0 a}. \tag{55}$$

Thus we find that the ratio of the TM shift to the TE shift at $k_0 a \gg 1$ is greater than unity for the first-order mode.

The solid curves in Fig. 1 are plots of sensitivity factor $f_{\mathrm{TE}} \equiv -(\Delta k/k_0)_{\mathrm{TE}}/[m_2 \Delta m_2 ({m_1}^2 - {m_2}^2)^{-1}]$ for the first, second, and third-order modes ($n = 1, 2, 3$, respectively) as a function of size parameter $k_0 a$. Dashed curves depict $f_{\mathrm{TM}} \equiv -(\Delta k/k_0)_{\mathrm{TM}}/[m_2 \Delta m_2 ({m_1}^2 - {m_2}^2)^{-1}]$; equations (47) and (48) with $m_1 = 1.47$ (silica) and $m_2 = 1.33$ (water) were used for the calculation. For reference, approximate formulas (54) and (55) are also shown in Fig. 1, as dashed–dotted curves. At $k_0 a \gg 1$, both f_{TE} and f_{TM} decrease as $\sim(k_0 a)^{-1}$ and run close to the approximate formulas. In this range, $f_{\mathrm{TE}} < f_{\mathrm{TM}}$ for each mode. The higher-order mode (greater n) experiences a greater shift at the same $k_0 a$, but the difference quickly disappears with increasing $k_0 a$. Both f_{TE} and f_{TM} peak

near $k_0a \cong 76$ for the first-order mode. The peak is due to a term neglected in formulas (52) and (53): The peak moves left and up, extending the nearly straight section, when m_1 is increased, thus more strongly confining the resonant photon by a greater contrast of refractive index.

For a given sphere with $a/\lambda \gg 1$, $\Delta k/k_0$ is proportional to wavelength λ. The shorter the wavelength, the weaker is the effect of the surroundings. This fact is related to the penetration depth of the evanescent field from a medium with a high refractive index to a medium with a low refractive index when total internal reflection occurs. In fact, the reciprocal of the decay rate of $S_l(r)$ and $T_l(r)$ for $l \gg 1$ at $r = a_+$, where a_+ is infinitesimally greater than a, is identical to the penetration depth.

Toward the low end of k_0a in Fig. 1 the sensitivity factor is high, but the resonance peak is too broad for any meaningful detection of Δm_2 by measurement of $\Delta k/k_0$. We can arbitrarily set the detection limit to width w of the peak (in terms of k_0a), which is given by[13]

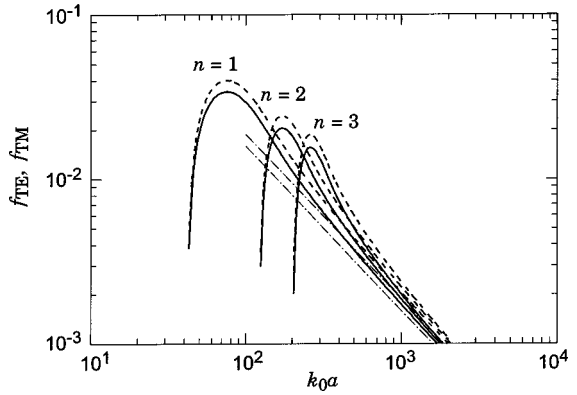

Fig. 1. Sensitivity f_{TE} (solid curves) and f_{TM} (dashed curves) of the resonance frequencies of TE and TM modes, respectively, in a microsphere to a uniform refractive-index change in the surrounding medium, plotted as a function of size parameter k_0a. These curves are for the first three orders ($n = 1, 2, 3$) for $m_1 = 1.47$ and $m_2 = 1.33$. Dashed–dotted curves represent approximations [formulas (54) and (55)]; the lower curve represents f_{TE}.

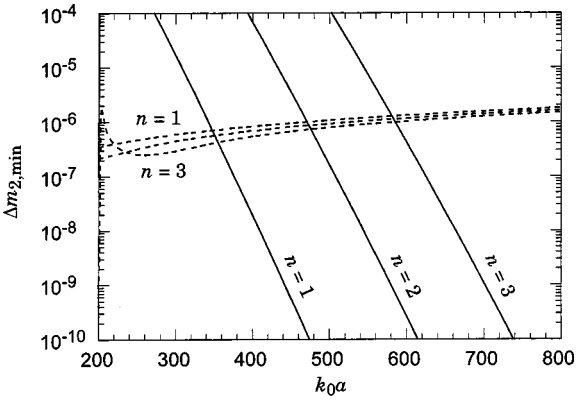

Fig. 2. Expected sensing limit $\Delta m_{2,min}$ of refractive-index change in the surrounding medium in microspheres of different values of k_0a for the first three modes. Solid curves are from the intrinsic linewidth of resonance; dashed curves denote the sensing limit for the current distributed-feedback laser driver's resolution, $\Delta k/k_0 = 10^{-8}$.

$$w = \frac{2m_2}{{m_1}^2 - {m_2}^2} \frac{1}{[\chi_l(m_2k_0a)]^2} \tag{56}$$

for the TE mode. The actual detection limit is much lower.[4] Then the smallest $\Delta m_{2,min}$ that can be detected is estimated as

$$\Delta m_{2,min} = 2/(k_0a\chi_l{}^2 f_{TE}) = 2/[k_0a(\chi_{l+1}\chi_{l-1} - \chi_l{}^2)]. \tag{57}$$

Likewise, for the TM mode,

$$\Delta m_{2,min} = \frac{2}{k_0a\chi_l{}^2} \frac{1}{(l + {}^1/_2)^2/(m_1k_0a)^2 + (\chi_l'/\chi_l)^2}. \tag{58}$$

The solid curves in Fig. 2 show $\Delta m_{2,min}$ for the first three orders of the TE mode. We have found that the first-order mode is the most sensitive at the same value of k_0a. At $k_0a = 400$, $\Delta m_{2,min}$ as small as 2×10^{-8} can be detected. We also found that $\Delta m_{2,min}$ decreases rapidly with increasing k_0a, which is due to smaller leakage of the photon energy.

There is another limit on $\Delta m_{2,min}$ that is due to a finite laser linewidth or fluctuations in the source wavelength, whichever is greater. In the study of protein adsorption[3,4] a distributed-feedback laser ($\lambda = 1.34\ \mu$m) was used. It was found that the source wavelength fluctuations surpass the laser linewidth. The fluctuations were $\sim 10^{-5}$ nm, which translates to $\Delta k/k_0 \sim 10^{-8}$. The dashed curves in Fig. 2 represent $\Delta m_{2,min}$ imposed by this restriction. They are nearly flat from $\sim 10^{-6}$ to $\sim 10^{-7}$ in the range of the figure. It is now apparent that the second limit poses severe restrictions on the detection limit. Efforts are under way to decrease the source fluctuations.

B. Adsorption of Molecules in a Thin Layer

Small molecules with a small excess isotropic polarizability α_{ex} are adsorbed at a uniform surface density σ on the exterior side of the surface of a sphere immersed in a solvent with refractive index m_2. Refractive-index change δm_2 caused by the adsorption is given as

$$\delta m_2 = \frac{\alpha_{ex}\sigma}{2\varepsilon_0 m_2}\,\delta(r - a_+). \tag{59}$$

Then

$$\langle k_0|m\,\delta m|k_0\rangle = \frac{\alpha_{ex}\sigma}{2\varepsilon_0}[B_l(k)]^2\phi_l{}^2 \tag{60}$$

for the TE mode. The fractional frequency shift of the mode is

$$\left(\frac{\Delta k}{k_0}\right)_{TE} = -\frac{\alpha_{ex}\sigma}{\varepsilon_0 a} \frac{1}{{m_1}^2 - {m_2}^2}. \tag{61}$$

Note that the fractional frequency shift is flat for all values of k_0a and is common to all orders. The same result was obtained by Arnold *et al.*, who used the energy perturbation approach.[4]

For the TM mode we use the general formula given by Eq. (45). The integral is

$$\int \frac{\delta m}{m^3}\left[\left(\frac{dT_0}{dr}\right)^2 + \frac{l(l+1)}{2}T_0^2\right]dr = \frac{\alpha_{ex}\sigma}{2\varepsilon_0 m_2^2}k_0^2[A_l(k_0)]^2\chi_l^2\left[\frac{l(l+1)}{(m_2k_0a)^2} + \left(\frac{\chi_l'}{\chi_l}\right)^2\right]. \quad (62)$$

Then the fractional frequency shift is given as

$$\left(\frac{\Delta k}{k_0}\right)_{TM} = \left(\frac{\Delta k}{k_0}\right)_{TE}\frac{l(l+1)/(m_2k_0a)^2 + (\chi_l'/\chi_l)^2}{l(l+1)/(m_1k_0a)^2 + (\chi_l'/\chi_l)^2}. \quad (63)$$

Because $m_1 > m_2$, $(\Delta k/k_0)_{TM}/(\Delta k/k_0)_{TE} > 1$. Adsorption of molecules with isotropic polarizability causes a greater shift in the TM mode than it does in the TE mode.

For $l \gg 1$ the use of Eq. (B5) below leads to the following revision of Eq. (63):

$$\left(\frac{\Delta k}{k_0}\right)_{TM}\Big/\left(\frac{\Delta k}{k_0}\right)_{TE} \cong \frac{2(l/m_2k_0a)^2 - 1}{(1 + m_2^2/m_1^2)(l/m_2k_0a)^2 - 1}. \quad (64)$$

We can further simplify formula (64) for the first-order mode:

$$\left(\frac{\Delta k}{k_0}\right)_{TM}\Big/\left(\frac{\Delta k}{k_0}\right)_{TE} \cong 2 - \left(\frac{m_2}{m_1}\right)^2. \quad (65)$$

It is easy to extend the results obtained here to the frequency shifts that are due to coating of the sphere's surface with a thin layer of thickness t ($t \ll \lambda$). For the refractive-index change Δm_2 in the coating, the fractional frequency shift of the TE mode is

$$\left(\frac{\Delta k}{k_0}\right)_{TE} = -\frac{2m_2\Delta m_2}{a(m_1^2 - m_2^2)}t, \quad (66)$$

where $\alpha_{ex}\sigma/(2\varepsilon_0) = m_2\Delta m_2 t$ was used. For the TM mode, the shift is given by Eqs. (63) and (66).

The frequency shift that is due to the coating depends on $t\Delta m_2$ proportional to the total mass of the coating material excluding the solvent in the layer. This result leads to the following situation: If the coating is a polymer brush grafted onto the sphere's surface or a polymeric gel, a change in thickness does not change the resonance frequency as long as the coating remains sufficiently thin. A change in thickness can be caused by a change in the environment, e.g., in temperature or in pH. When a change in thickness is caused by adsorption of a second substance, it is only the second substance that changes its resonance frequency. Conformational changes of the brushes that may occur concomitantly with adsorption will not affect the resonance. Thus we detect the adsorbed second substance only.

Apparently our formulation does not apply to a large perturbation that causes the refractive index of the coating to increase to a level close to m_1. This is clear when we consider a situation in which a thin layer of refractive index m_1 is added to the sphere, effectively increasing the sphere's radius. The resonance condition states that k_0a be held constant for TE and TM modes under this perturbation; Eq. (66) contradicts this supposition. This inconsistency comes from a limitation of our first-order perturbation approach. For the TE mode we can have a consistent formula for $\Delta k/k_0$ by considering $\delta(m^2)$, the change in the relative permittivity, in place of δm in our first-order perturbation theory. The result is identical to the one obtained by Folan[15] and presented in Ref. 8. For the TM mode this modification falls short, because the exact formula[15] is a nonlinear function of $\delta(m^2)$. We intend to address this problem in a future publication. It is to be noted here that the TM shift given by Eqs. (63) and (66) [$m_2\Delta m_2$ replaced by $\Delta(m_2^2)/2$] is identical to the linear part of the exact formula.

When the refractive-index change occurs in the interior side of the interface, the frequency shift of the TE mode is the same as that given by Eq. (61), but it is different for the TM mode. Now it is

$$\left(\frac{\Delta k}{k_0}\right)_{TM} = \left(\frac{\Delta k}{k_0}\right)_{TE}\frac{l(l+1)/(m_1k_0a)^2 + (\psi_l'/\psi_l)^2}{l(l+1)/(m_2k_0a)^2 + (\psi_l'/\psi_l)^2}, \quad (67)$$

where $\psi_l(z)$ and $\psi_l'(z)$ are evaluated at $z = m_1k_0a$. The TM shift is smaller.

C. Depletion of Refractive Index at the Interface

We have learned in example (A) above that the sensitivity of the resonance shift to the refractive-index change or the surrounding medium depends on k_0a. Then we can expect that using different values of k_0a and especially of λ will enable a WGM to be a sensor for the refractive-index profile of the surrounding medium near the surface. When the exterior medium is a solution of macromolecules or a suspension of particles, the refractive index of the solution will change as a function of the distance from the sphere surface. If the solute has a positive differential refractive index and does not interact with the microsphere except to create a steric hindrance (excluded volume), the refractive index will have the profile depicted in Fig. 3. This mean-field refractive-index profile may not be valid for suspension of large solid particles with a large refractive-index difference but will be a good approximation for solutions of macromolecules and suspensions of swollen gel particles and vesicles.

It is convenient to separate $\Delta m_2(r)$ into two parts: $\Delta m_2(r) = \Delta m_2(\infty) - [\Delta m_2(\infty) - \Delta m_2(r)]$. In the first-order perturbation, each term gives an independent frequency shift. Thus

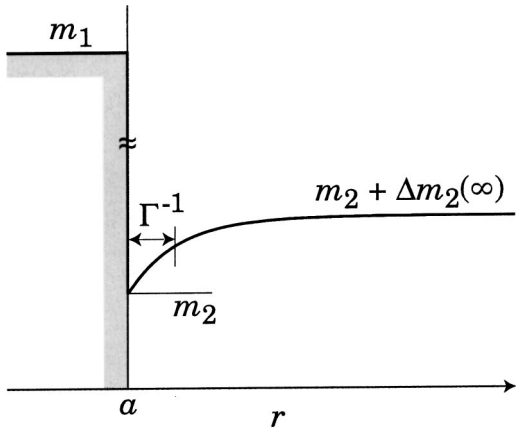

Fig. 3. Refractive-index profile across the interface surrounding a microsphere.

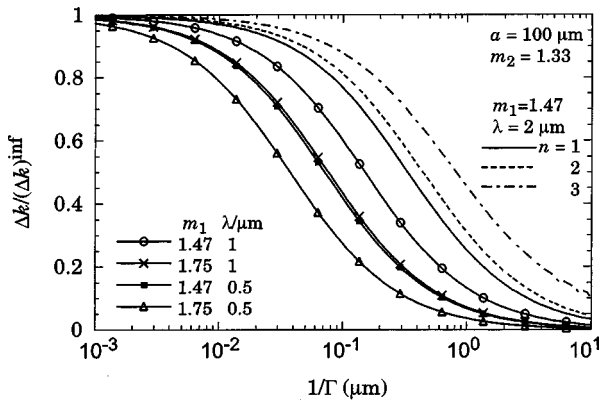

Fig. 4. Frequency shift as a result of a refractive-index change of $\Delta m_2(r) = \Delta m_2(\infty)\{1 - \exp[-\Gamma(r-a)]\}$ reduced by the shift that is due to a constant Δm_2, plotted as a function of $1/\Gamma$.

$$\frac{\Delta k}{k_0} = \left(\frac{\Delta k}{k_0}\right)^{\inf} - \left(\frac{\Delta k}{k_0}\right)^{\mathrm{dep}}, \tag{68}$$

where the first term is given by Eqs. (47) and (48) [$\Delta m_2(\infty)$ in place of Δm_2] for the TE and TM modes, respectively. The second term decreases rapidly to zero at long distances. For the TE mode

$$\left(\frac{\Delta k}{k_0}\right)^{\mathrm{dep}}_{\mathrm{TE}} = -\frac{\langle k_0|m_2[\Delta m_2(\infty) - \Delta m_2(r)]|k_0\rangle}{\langle k_0|m_2{}^2|k_0\rangle}$$

$$= -\frac{m_2\int_a^\infty [\chi_l(m_2k_0r)]^2[\Delta m_2(\infty) - \Delta m_2(r)]\mathrm{d}r}{(a/2)[\chi_l(m_2k_0a)]^2(m_1{}^2 - m_2{}^2)}. \tag{69}$$

For the TM resonance, $(\Delta k/k_0)^{\mathrm{dep}}_{\mathrm{TM}}$ can be calculated similarly from Eq. (45).

A numerical calculation was made for a profile $\Delta m_2(r)$ that changes as

$$\Delta m_2(r)/\Delta m_2(\infty) = 1 - \exp[-\Gamma(r-a)] \tag{70}$$

for $r > a$. The solid curves in Fig. 4 are plots of Δk of the first-order TE mode, reduced by $(\Delta k)^{\inf}$ for $a = 100\ \mu$m and $m_2 = 1.33$, but with various values of m_1 and λ. The dashed and dash–dotted curves are for higher-order modes ($n = 2,3$) with $m_1 = 1.47$ and $\lambda = 2\mu$m. Comparing the five solid curves, we can see that the shorter the wavelength or the greater the refractive index of a microsphere, the less is the sensitivity to deeper depression. A higher-order mode with greater n can explore a deeper depression. The values of parameters used in the figure are currently accessible in practice. Use of microsphere sensors of different values of λ and m_1 and analyses of various orders of resonance will allow us to estimate the depth of depression and its profile. In a solution of macromolecules, for instance, we should be able to find the molecular weight distribution just by dipping the sensor heads into the solution. A more elaborate expression for $\Delta m_2(r)$ is necessary for that purpose.

6. CONCLUSIONS

We used first-order perturbation theory to obtain formulas for the resonance frequency shift that is due to refractive-index variations in a medium exterior to a microsphere, and we applied the general formulas to three examples. The first example can be used to construct tiny refractive-index detectors that may replace the bulky detectors that are widely used in liquid chromatography. The third example paves the way for small instruments to measure size distributions of suspensions and molecular weight distributions of polymers; the measurement will be instantaneous. The second example exposed a limit of our first-order perturbation theory; here a different approach is needed.

In this paper we did not consider an equally important microsphere system that has a decaying WGM. It will be possible to extend our first-order perturbation theory to a system with a complex frequency. A slightly different formulation may be needed. Then the effects of environmental change, including imaginary Δm_2, on the resonance linewidth can be treated. We intend to address this problem in future publications.

APPENDIX A: INTEGRALS IN NORMALIZATION

We evaluate the two integrals in Eq. (21). Let $k_a = k + \Delta k$. For a small $m_1a\Delta k$,

$$\psi_l(m_1k_aa) = \psi_l(m_1ka) + m_1a\Delta k\psi_l{}'(m_1ka), \tag{A1}$$

$$\psi_l{}'(m_1k_aa) = \psi_l{}'(m_1ka) + m_1a\Delta k\left[\frac{l(l+1)}{(m_1ka)^2} - 1\right]\psi_l(m_1ka), \tag{A2}$$

where Eq. (7) has been used. Then the upper limit of the first integral is

$$\lim_{\Delta k\to 0m_1}\frac{1}{(k^2 - k_a{}^2)}[-k\psi_l{}'(m_1ka)\psi_l(m_1k_aa) + k_a\psi_l(m_1ka)\psi_l{}'(m_1k_aa)]$$

$$= -\frac{1}{2m_1k}\left\{-m_1ak\psi_l{}'^2 + \left[\frac{l(l+1)}{m_1ka} - m_1ka\right]\times\psi_l{}^2 + \psi_l\psi_l{}'\right\}, \tag{A3}$$

where the Ricatti–Bessel functions are evaluated at $z = m_1ka$.

We need to be careful about the integral of $\phi_l(m_2kr)\phi_l(m_2k_ar)$ over (a, ∞) because $\phi_l(m_2kr)$ is a linear combination of χ_l and ψ_l with a k-dependent superposition coefficient. We note that

$$\phi_l(m_2k_aa) = \phi_l(m_2ka) + m_2a\Delta k\phi_l{}'(m_2ka) + \Delta k\beta_l{}'\psi_l(m_2ka), \tag{A4}$$

where the derivative of ϕ_l is defined for a constant β_l. Likewise,

$$\phi_l{}'(m_2k_aa) = \phi_l{}'(m_2ka) + m_2a\Delta k\times\left[\frac{l(l+1)}{(m_2ka)^2} - 1\right]\phi_l(m_2ka) + \Delta k\beta_l{}'\psi_l{}'(m_2ka). \tag{A5}$$

Then the lower limit of the second integral in Eq. (21) is

$$\lim_{\Delta k\to 0}\frac{1}{m_2(k^2-k_a{}^2)}[-k\phi_l'(m_2ka)\phi_l(m_2k_aa) + k_a\phi_l(m_2ka)\phi_l'(m_2k_aa)] = -\frac{1}{2m_2k}\left\{-m_2ka\,\phi_l{}'^2+\left[\frac{l(l+1)}{m_2ka}-m_2ka\right]\times\phi_l{}^2+\phi_l\phi_l'\right\}+\frac{\beta_l'}{2m_2}, \quad \text{(A6)}$$

where ϕ_l and ϕ_l' are evaluated at $z = m_2ka$ and Eq. (C5) below has been used.

The upper limit of the integral is evaluated in the same way. We use $\psi_l(z)\cong\sin(z-l\pi/2)$ and $\chi_l(z)\cong-\cos(z-l\pi/2)$ for large z. A lengthy calculation leads to

$$\lim_{\Delta k\to 0}\frac{1}{m_2(k^2-k_a{}^2)}\lim_{r\to\infty}[k\phi_{l+1}(m_2kr)\phi_l(m_2k_ar) - k_a\phi_l(m_2kr)\phi_{l+1}(m_2k_ar)] = \beta_l'/2m_2, \quad \text{(A7)}$$

where sinusoidal functions have been set to zero. Combining Eqs. (A3), (A6), and (A7), we have

$$\lim_{\Delta k\to 0}\int_0^\infty S_l(r,k)S_l(r,k+\Delta k)[m(r)]^2\mathrm{d}r = \psi_l{}^2(a/2)(m_1{}^2-m_2{}^2). \quad \text{(A8)}$$

We can use this result for normalization of $S_l(r,k)$. We write the integral as

$$\langle S_l|m^2|S_l\rangle = \psi_l{}^2\frac{a}{2}(m_1{}^2-m_2{}^2). \quad \text{(A9)}$$

For the TM mode

$$\langle T_l|T_l\rangle = \psi_l{}^2\frac{a}{2}\left(\frac{m_1{}^2}{m_2{}^2}-1\right)\left[\frac{l(l+1)}{(m_1ka)^2}+\left(\frac{\chi_l'}{\chi_l}\right)^2\right]. \quad \text{(A10)}$$

APPENDIX B: ASYMPTOTIC EXPANSION OF RICATTI–NEUMANN FUNCTIONS

In estimating $\chi_l'(z)$ for large l, the following asymptotic expansion of the Neumann function is useful:

$$N_\nu(\nu\,\mathrm{sech}\,s)\cong-\frac{\exp[\nu(s-\tanh s)]}{[(\pi/2)\nu\tan s]^{1/2}}, \quad \text{(B1)}$$

with $s>0$. The spherical Neumann function $n_l(z)$ is then expressed as

$$n_l(z)\cong-\left(l+\frac{1}{2}\right)^{-1}\times\exp\left[\left(l+\frac{1}{2}\right)(s-\tanh s)\right]\frac{\cosh s}{\sinh^{1/2}s}, \quad \text{(B2)}$$

where

$$z=\left(l+\frac{1}{2}\right)\mathrm{sech}\,s. \quad \text{(B3)}$$

Then the decay rate of $n_l(z)$ is calculated as

$$\frac{n_l'}{n_l}\cong-\frac{1}{z}\left\{\left[\left(l+\frac{1}{2}\right)^2-z^2\right]^{1/2}+\frac{1}{2}-\frac{1}{2}\left[\left(l+\frac{1}{2}\right)^2\Big/z^2-1\right]^{-1}\right\}, \quad \text{(B4)}$$

and the decay rate of $\chi_l(z)=zn_l(z)$ is calculated as

$$\frac{\chi_l'}{\chi_l}\cong-\frac{1}{z}\left\{\left[\left(l+\frac{1}{2}\right)^2-z^2\right]^{1/2}-\frac{1}{2}\left[1-z^2\Big/\left(l+\frac{1}{2}\right)^2\right]^{-1}\right\}. \quad \text{(B5)}$$

Another useful relationship for large l can be obtained in a similar way:

$$\frac{\chi_{l+1}(z)}{\chi_l(z)}=\frac{n_{l+1}(z)}{n_l(z)}\cong\frac{l+1/2}{z}+\left[\left(\frac{l+1/2}{z}\right)^2-1\right]^{1/2}. \quad \text{(B6)}$$

With Eq. (C6) below, the factor that appears in Eq. (47) is approximated as

$$\frac{\chi_{l-1}\chi_{l+1}}{\chi_l{}^2}-1\cong\left[\left(l+\frac{1}{2}\right)^2-(m_2k_0a)^2\right]^{-1/2}, \quad \text{(B7)}$$

Equation (B2) allows a rough estimate to be made of $n_l(m_2k_0a)$ at resonance. For the first-order mode, $\cosh s\cong m_1/m_2$, which is slightly greater than 1. Then $s\cong[2(m_1/m_2-1)]^{1/2}$ and $s-\tanh s\cong[2(m_1/m_2-1)]^{3/2}/3$, which is of the order of 1. Inasmuch as $l+1/2\gg 1$, $n_l(m_2k_0a)$ is dominated by the exponential factor. Therefore $n_l(m_2k_0a)\gg 1$ and $\chi_l(m_2k_0a)\gg 1$.

APPENDIX C: RICATTI–NEUMANN FUNCTIONS

Here are some recurrence formulas for Ricatti–Neumann functions:

$$\psi_l'(z)=\frac{l+1}{z}\psi_l(z)-\psi_{l+1}(z), \quad \text{(C1)}$$

$$\psi_{l-1}(z)+\psi_{l+1}(z)=\frac{2l+1}{z}\psi_l(z), \quad \text{(C2)}$$

$$\chi_l'(z)=\frac{l+1}{z}\chi_l(z)-\chi_{l+1}(z), \quad \text{(C3)}$$

$$\chi_{l-1}(z)+\chi_{l+1}(z)=\frac{2l+1}{z}\chi_l(z). \quad \text{(C4)}$$

$$\psi_l(z)\chi_l'(z)-\psi_l'(z)\chi_l(z)=1. \quad \text{(C5)}$$

Using these recurrence formulas, we can derive a useful expression:

$$\frac{l(l+1)}{z^2} - 1 + \frac{1}{z}\frac{\chi_l'}{\chi_l} - \left(\frac{\chi_l'}{\chi_l}\right)^2 = \frac{\chi_{l-1}\chi_{l+1}}{\chi_l^2} - 1 = \frac{1}{z}\frac{\chi_{l-1}}{\chi_l} + \frac{\mathrm{d}}{\mathrm{d}z}\frac{\chi_{l-1}}{\chi_l}. \quad \text{(C6)}$$

ACKNOWLEDGMENT

We acknowledge financial support from the National Science Foundation through grant BES0119273.

I. Teraoka's e-mail address is teraoka@poly.edu.

REFERENCES AND NOTES

1. A. Serpengüzel, S. Arnold, and G. Griffel, "Enhanced coupling to microsphere resonances with optical fibers," Opt. Lett. **20**, 654–656 (1995).
2. A. T. Rosenberger, J. P. Rezac, "Evanescent-wave sensor using microsphere whispering-gallery modes," in *Laser Resonators III*, A. V. Kudryashov and A. H. Paxton, eds., Proc. SPIE **3930**, 186–192 (2000).
3. F. Vollmer, D. Braun, A. Libchaber, M. Khoshsima, I. Teraoka, and S. Arnold, "Protein detection by optical shift of a resonant microcavity," Appl. Phys. Lett. **80**, 4057–4049 (2002).
4. S. Arnold, M. Khoshsima, I. Teraoka, S. Holler, and F. Vollmer, "Shift of whispering gallery modes in microspheres by protein adsorption," Opt. Lett. **28**, 272–274 (2003).
5. V. B. Braginsky, M. L. Gorodetsky, and V. S. Ilchenko, "Quality-factor and nonlinear properties of optical whispering-gallery modes," Phys. Lett. A **137**, 393–397 (1989).
6. C. C. Lam, P. T. Leung, and K. Young, "Explicit asymptotic formulas for the positions, widths, and strengths of resonances in Mie scattering," J. Opt. Soc. Am. B **9**, 1585–1592 (1992).
7. G. Griffel, S. Arnold, D. Taskent, A. Serpenguezel, J. Connolly, and D. G. Morris, "Morphology-dependent resonances of a microsphere-optical fiber system," Opt. Lett. **21**, 695–697 (1996).
8. M. L. Gorodetsky, A. A. Savchenkov, and V. S. Ilchenko, "Ultimate *Q* of optical microsphere resonators," Opt. Lett. **21**, 453–455 (1996).
9. V. S. Ilchenko, X. S. Yao, and L. Maleki, "Pigtailing the high-*Q* microsphere cavity: a simple fiber coupler for optical whispering-gallery modes," Opt. Lett. **24**, 723–725 (1999).
10. P. J. Wyatt, "Scattering of electromagnetic plane waves from inhomogeneous spherically symmetric objects," Phys. Rev. **127**, 1837–1843 (1962).
11. D. Q. Chowdhury, S. C. Hill, and P. W. Barber, "Morphology-dependent resonances in radially inhomogeneous spheres," J. Opt. Soc. Am. A **8**, 1702–1705 (1991).
12. H. M. Lai, P. T. Leung, K. Young, P. W. Barber, and S. C. Hill, "Time-independent perturbation for leaking electromagnetic modes in open systems with application to resonances in microdroplets," Phys. Rev. A **41**, 5187–5198 (1990).
13. B. R. Johnson, "Theory of morphology-dependent resonances: shape resonances and width formulas," J. Opt. Soc. Am. A **10**, 343–352 (1993).
14. A typographical error in Ref. 13 [Eq. (5b)] was corrected.
15. L. M. Folan, "Characterization of the accretion of material by microparticles using resonant ellipsometry," Appl. Opt. **31**, 2066–2071 (1992).